Supplementary information

Total figures S1 to S37

Supplementary information **Figure S1.**

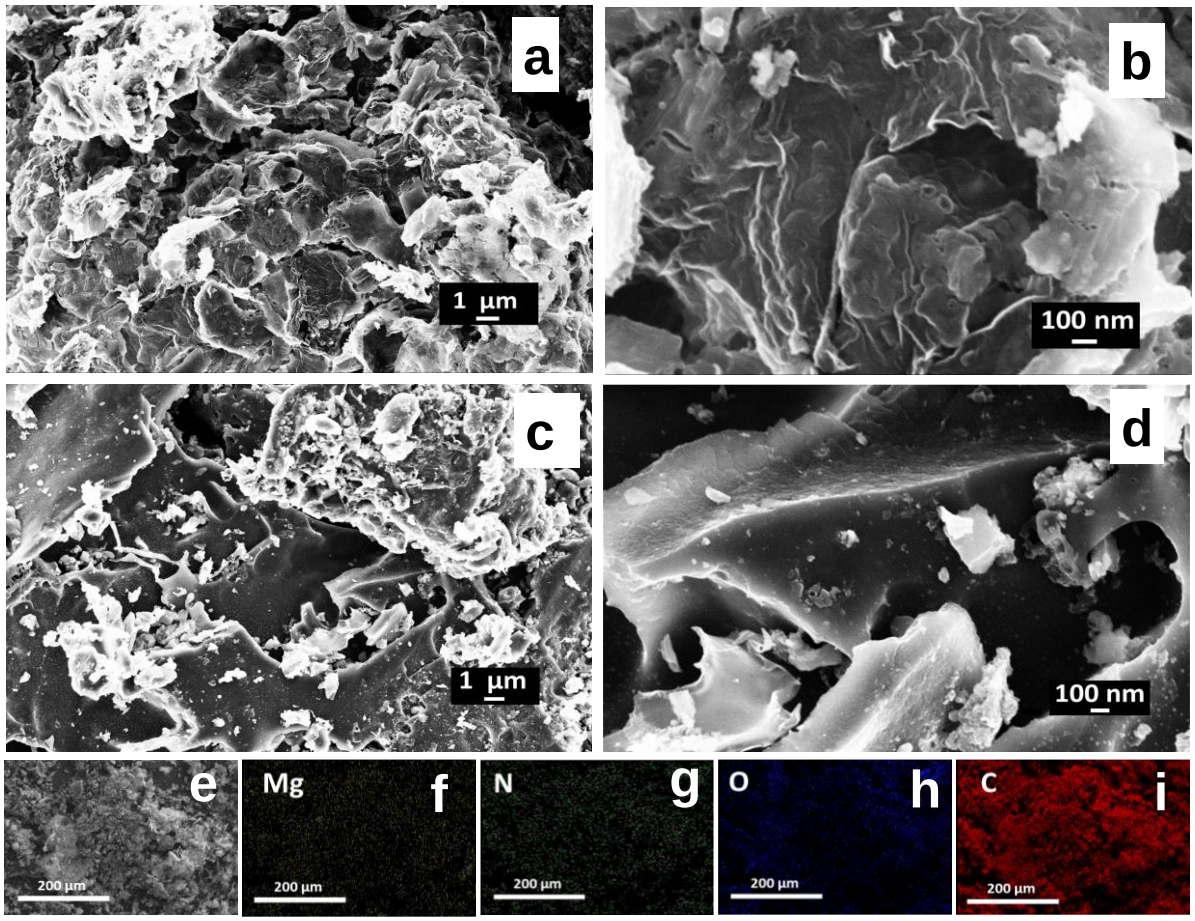

Figure. S1. SEM images of MgNxC650 (a-b), MgNxC850 (c-d) and different magnifications and EDS mapping of MgNxC650 with (e) Selected region, (f-i) for Mg, N, O, and C respectively.

Supplementary information **Figure S2.**

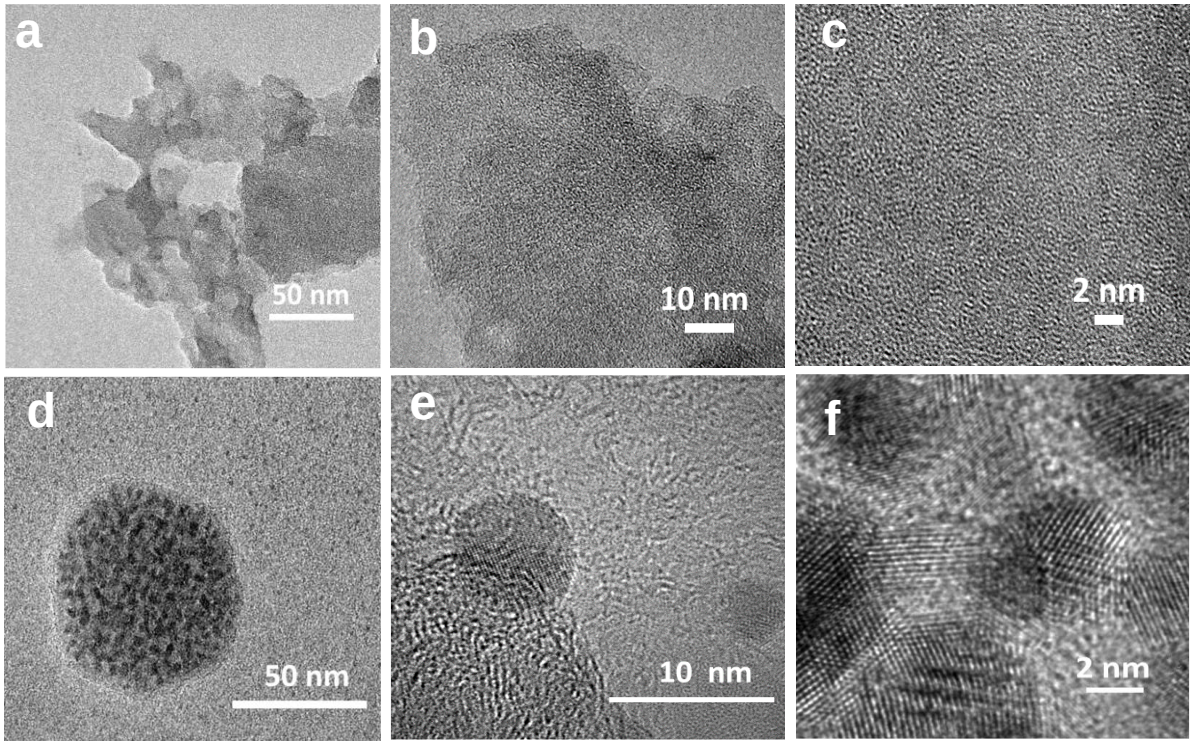

Figure. S2. HRTEM images at different magnifications of (a-c) MgNxC650 and (d-f) MgNxC850.

Supplementary information **Figure S3.**

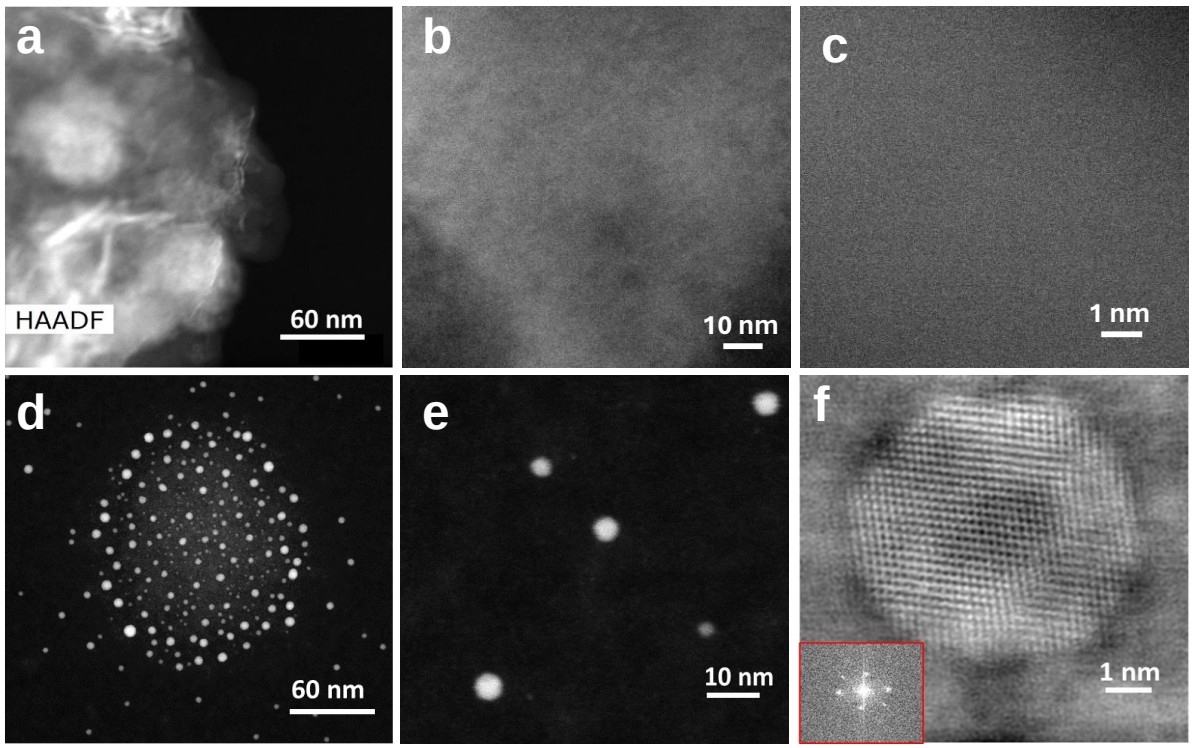

Figure. S3. HAADF-STEM EDS imaging of (a-c) MgNxC650, and (d-f) MgNxC850.

Supplementary information **Figure S4.**

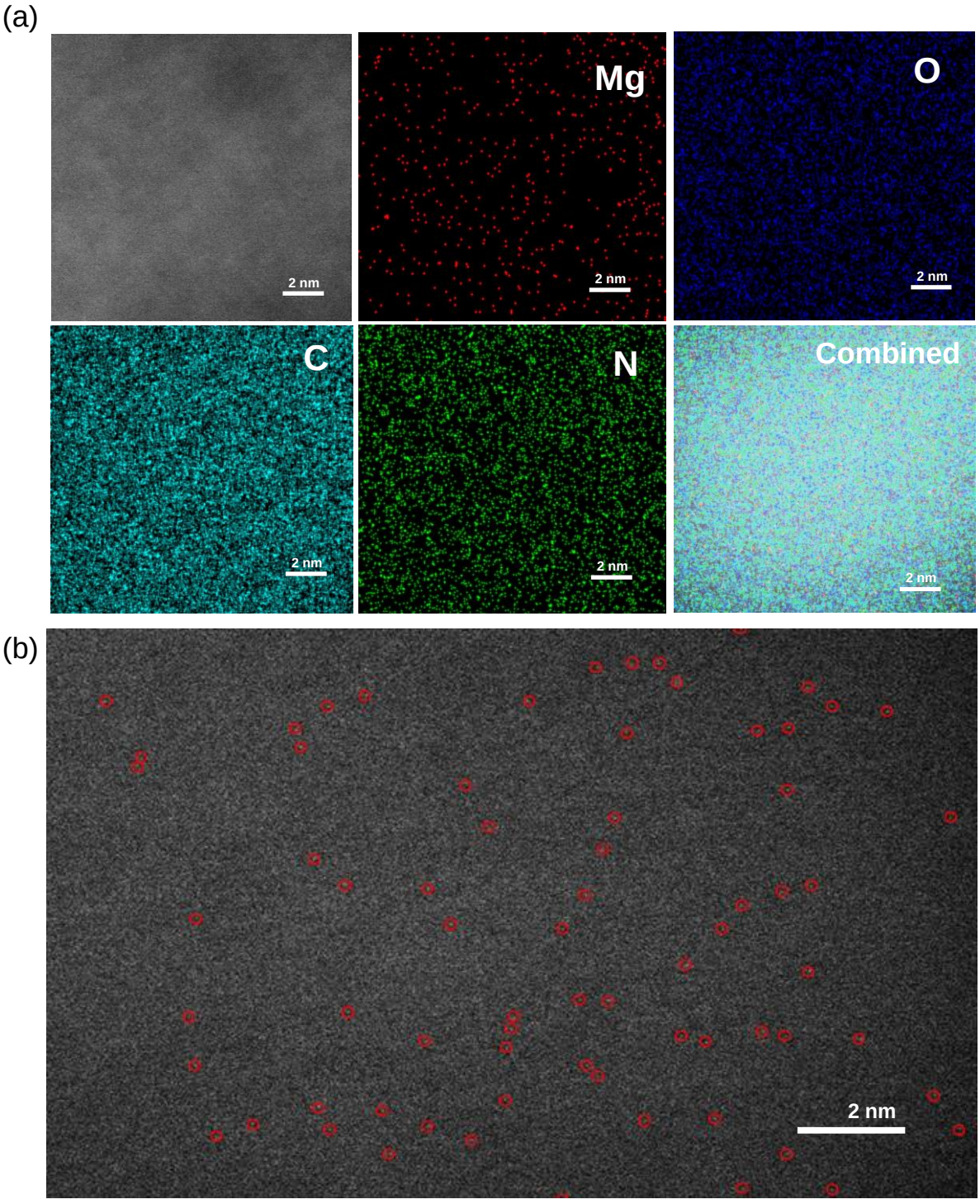

Figure. S4. The scale bar of 2 nm shows (a) Elemental mapping of elements and (b) atomic dispersion of magnesium atoms of MgNxC650.

Supplementary information **Figure S5.**

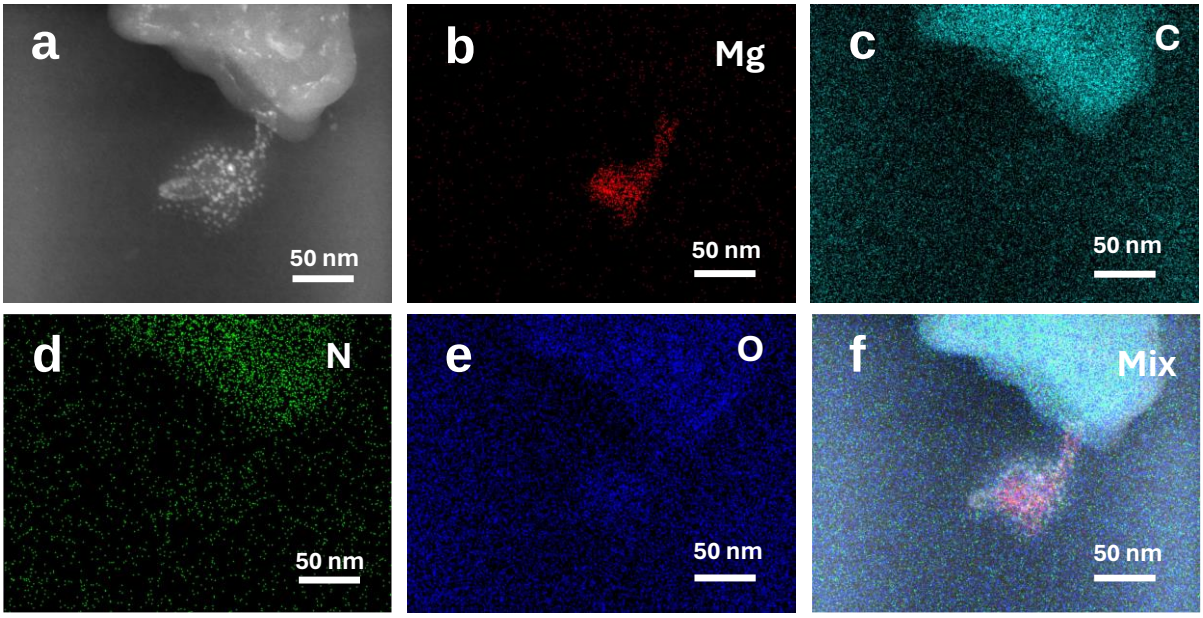

Figure. S5. HAADF-STEM EDS elemental mapping of MgNxC850 (a) region of interest, (b) Mg, (c) C, (d) N, (e) O, and (f) mixed depiction of the distribution of respective elements.

Supplementary information **Figure S6.**

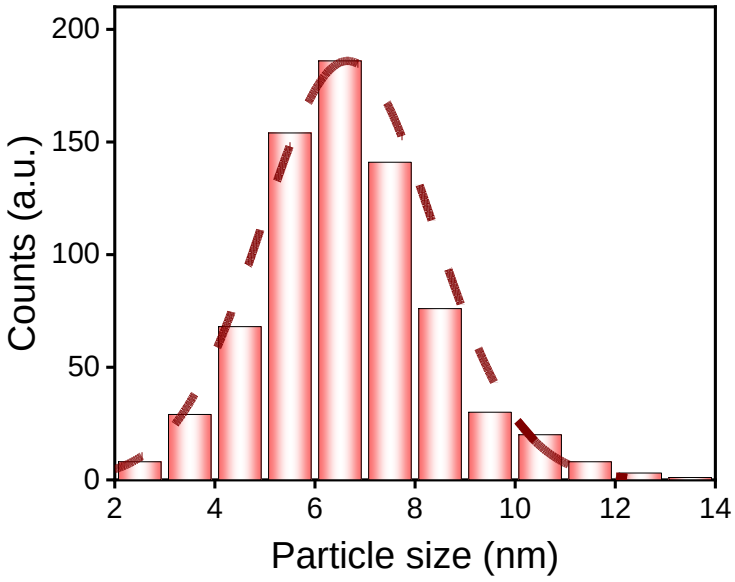

Figure. S6. Particle distribution of nanoparticle in MgNxC850 catalyst.

Supplementary information **Figure S7.**

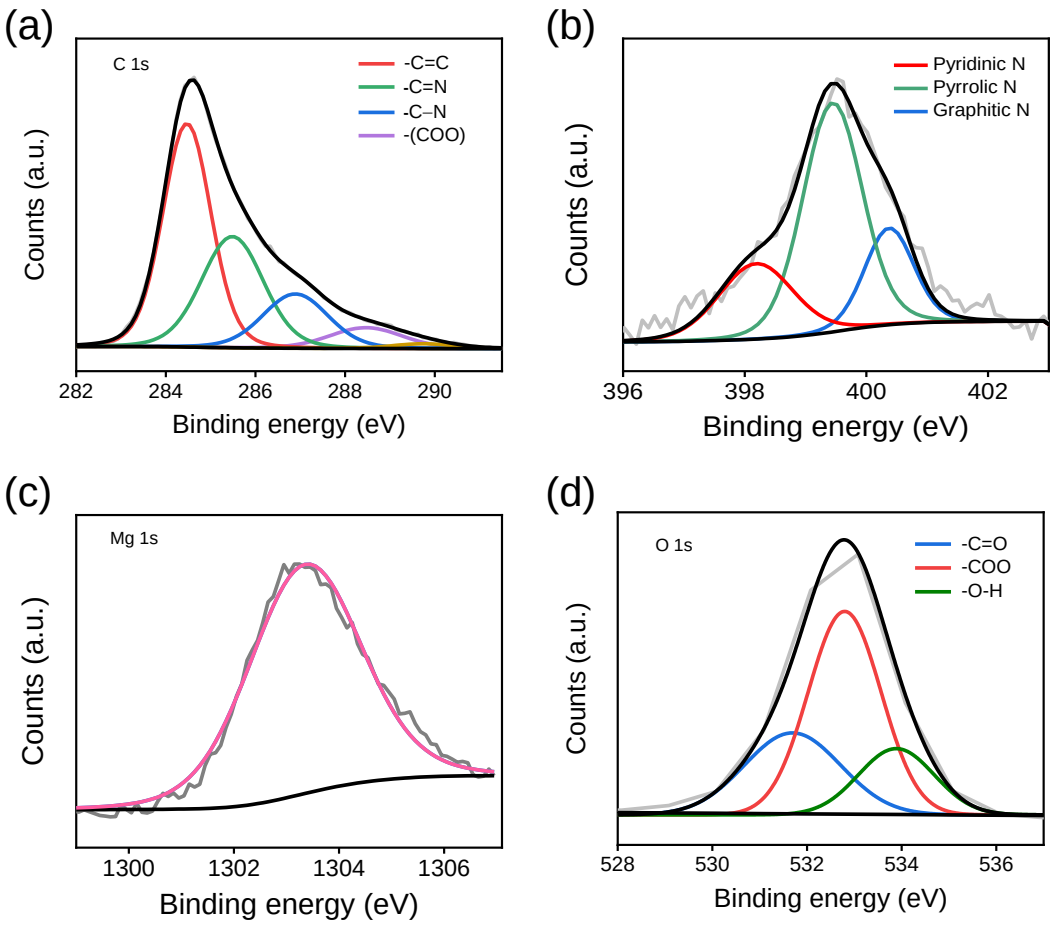

Figure. S7. XPS analysis of MgNxC850 with (a) C 1s, (b) N 1s, (c) Mg 1s and (d) O 1s spectra.

Supplementary information **Figure S8.**

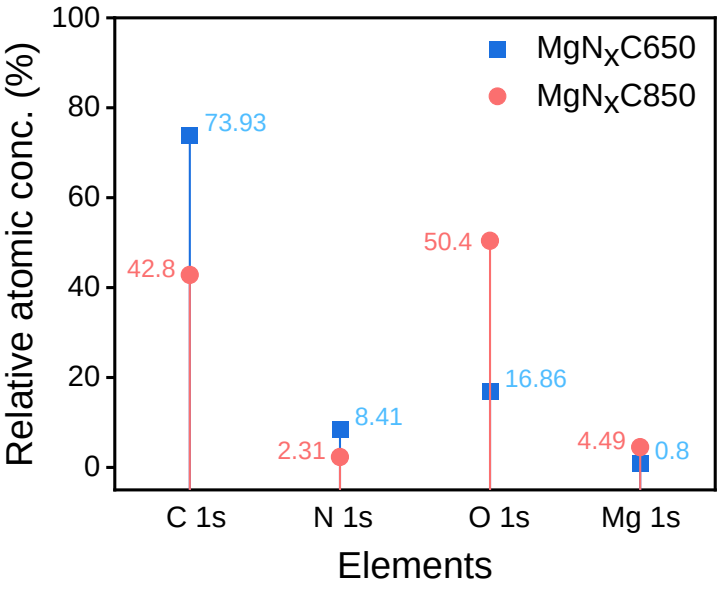

Figure. S8. Relative atomic concentrations (%) for MgNxC650 and MgNxC850 as respective elements.

Supplementary information **Figure S9.**

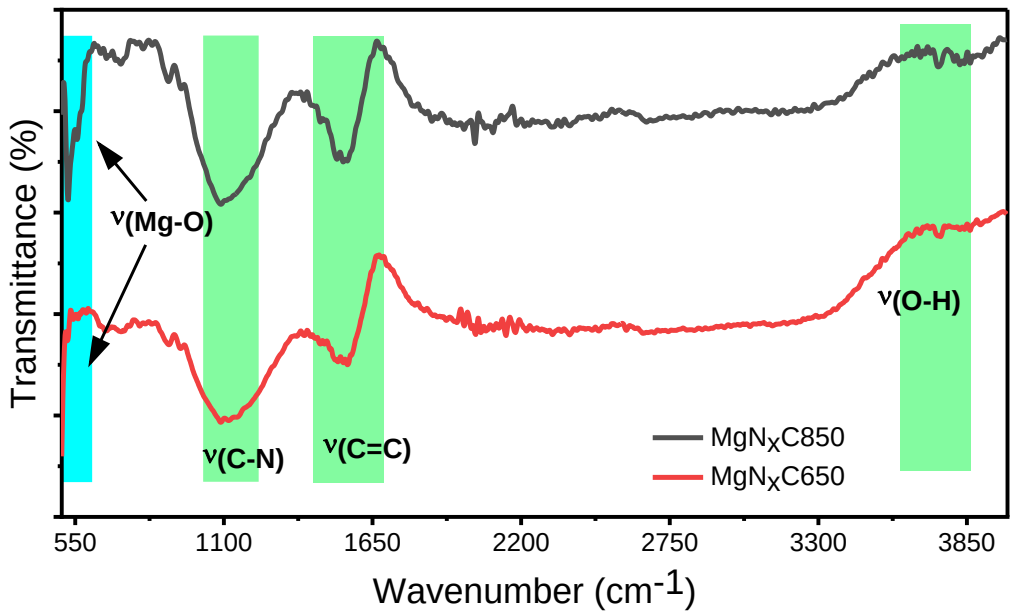

Figure. S9. FTIR spectrum of MgNxC650 and MgNxC850 , peak at near 550 cm^{-1} for stretching frequency of Mg-O bond.

Supplementary information **Figure S10.**

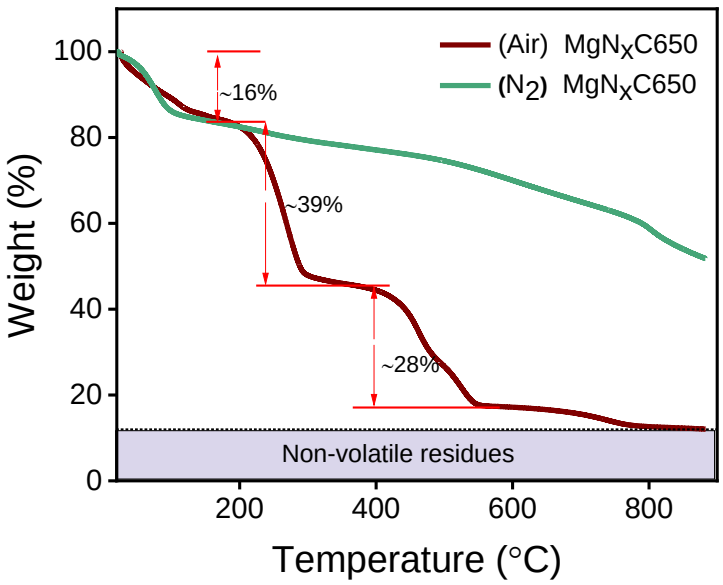

Figure. S10. Thermogravimetric analysis (TGA) performed in different environmental controlled media on MgNxC650.

Supplementary information **Figure S11.**

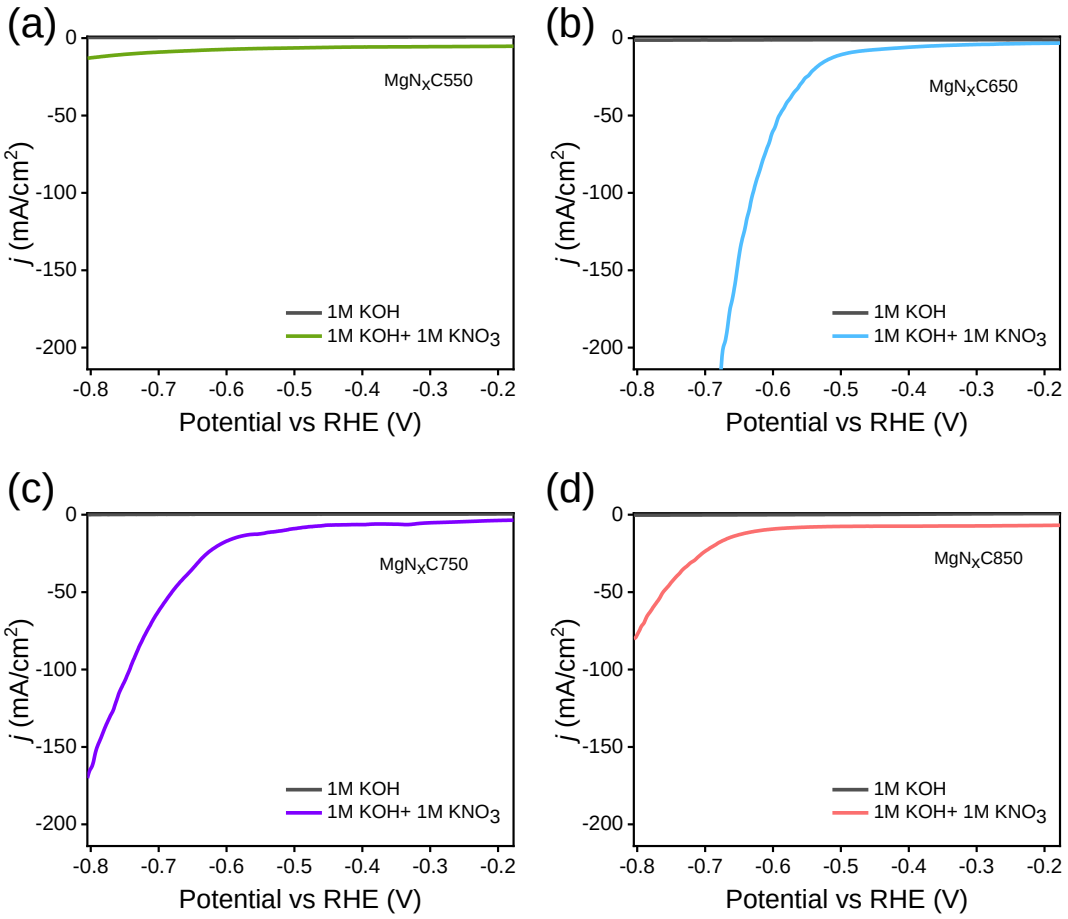

Figure. S11. Linear sweep voltammetry (LSV) measurements for MgNxC catalysts with and without nitrate source.

Supplementary information **Figure S12.**

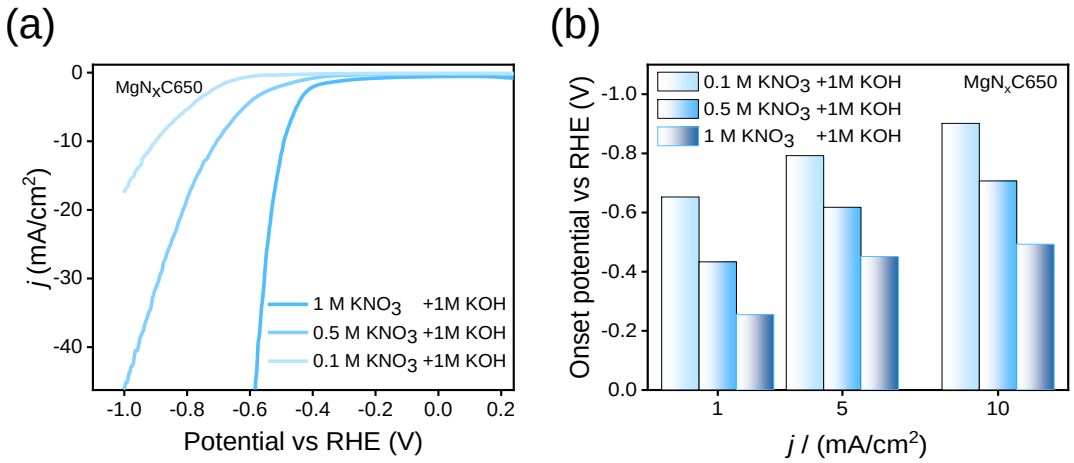

Figure. S12. (a) Different concentrations of nitrate source, and (b) Onset potential and overpotential vs RHE (V).

Supplementary information **Figure S13.**

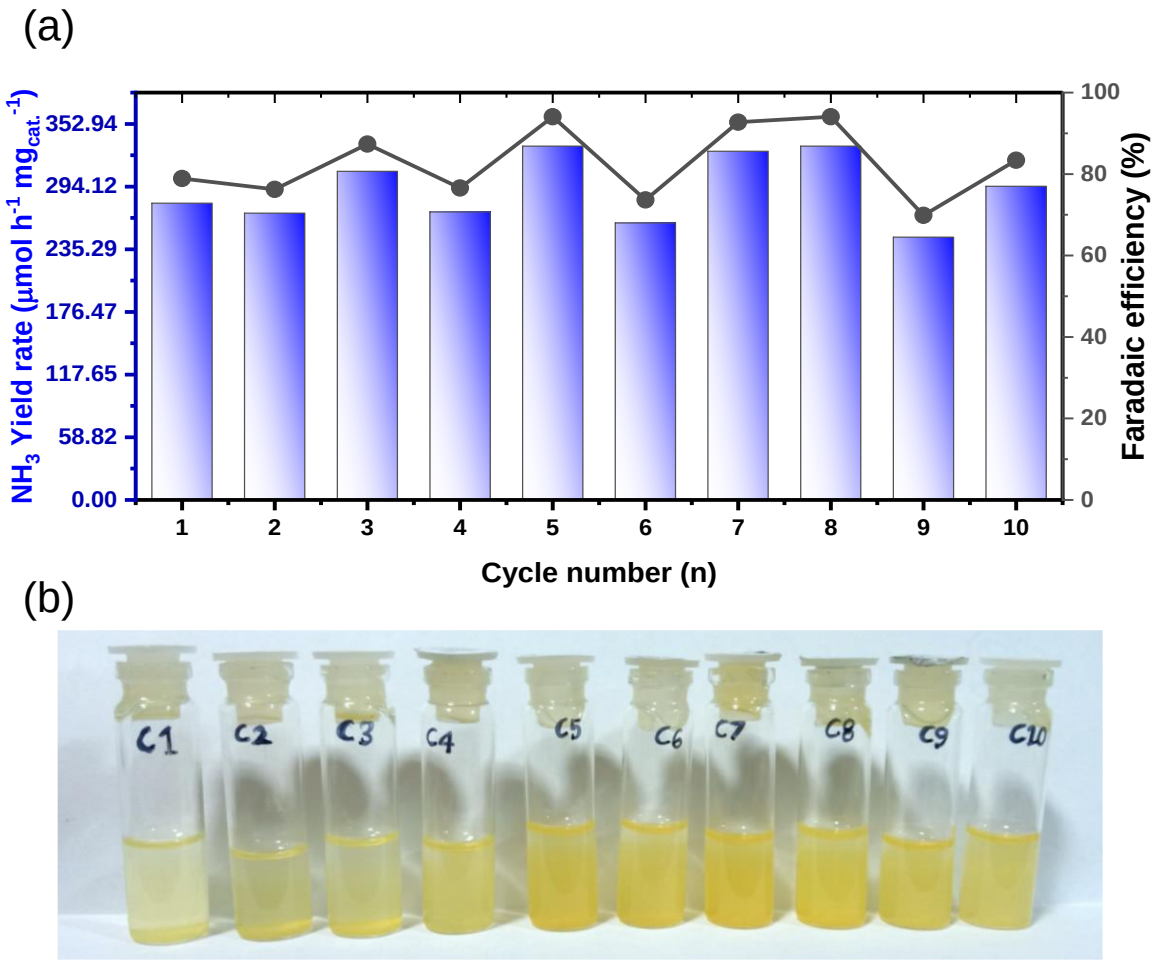

Figure. S13. Cyclic test performed for 30 minutes each for 5 hours showing repeatability by MgNxC650 at -0.58 vs RHE (V).

Supplementary information **Figure S14.**

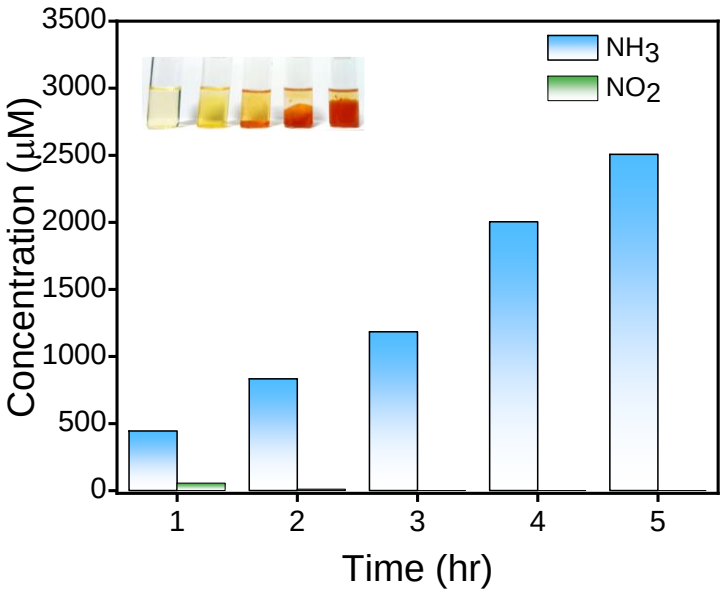

Figure. S14. Time-dependent studies for continuous for five hours using MgNxC650 at -0.58 vs RHE (V) toward ammonia production.

Supplementary information **Figure S15.**

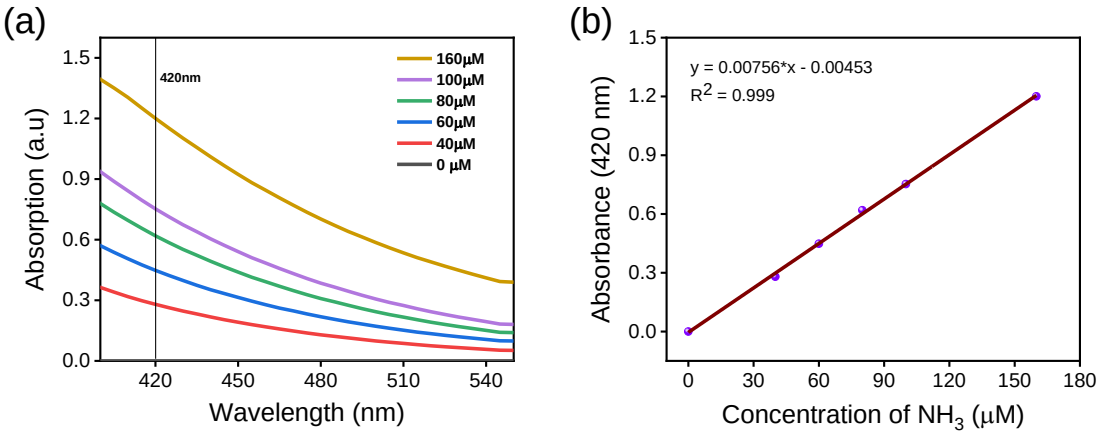

Figure. S15. (a) UV-Visible spectrum and (b) Calibration curve plot for estimation of NH_4^+ ion.

Supplementary information **Figure S16.**

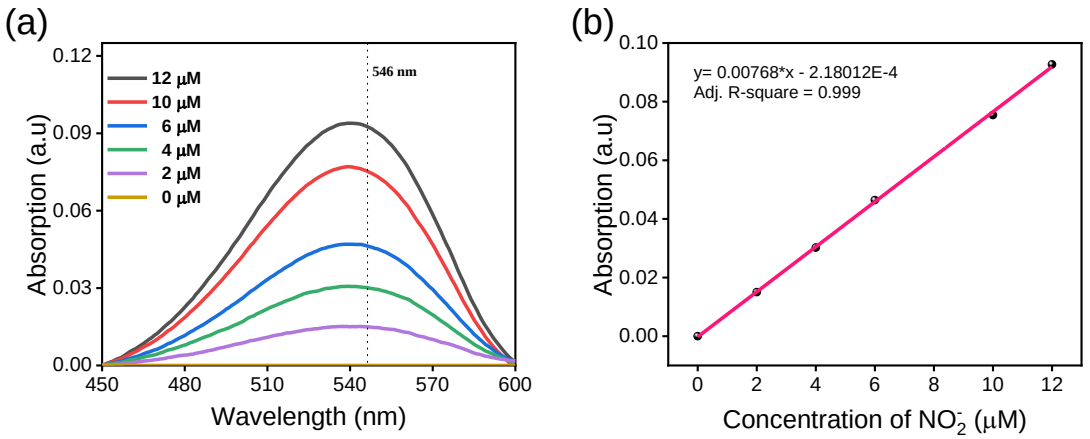

Figure. S16. (a) UV-Visible spectrum and (b) Calibration curve plot for the estimation of NO_2^- ion.

Supplementary information **Figure S17.**

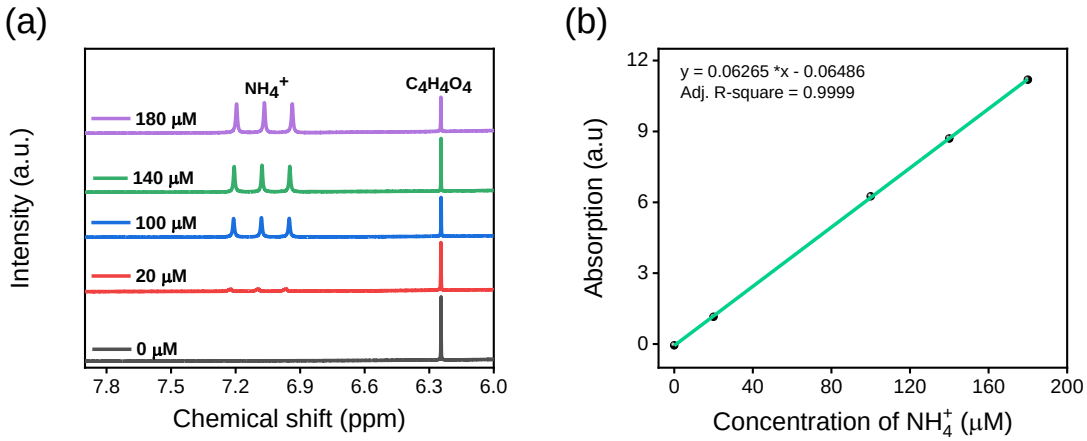

Figure. S17. (a) NMR response at different NH_4^+ concentrations and (b) Calibration curve plot for the estimation of NH_4^+ ion using NMR. spectroscopy.

Supplementary information **Figure S18.**

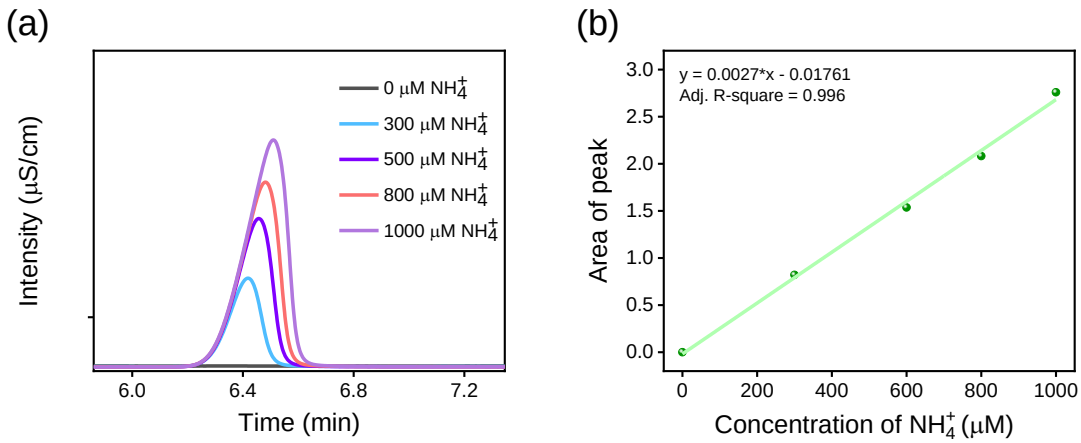

Figure. S18. (a) Ion-exchange chromatograms, and (b) Calibration curve plot for the estimation of NH_4^+ ion.

Supplementary information **Figure S19.**

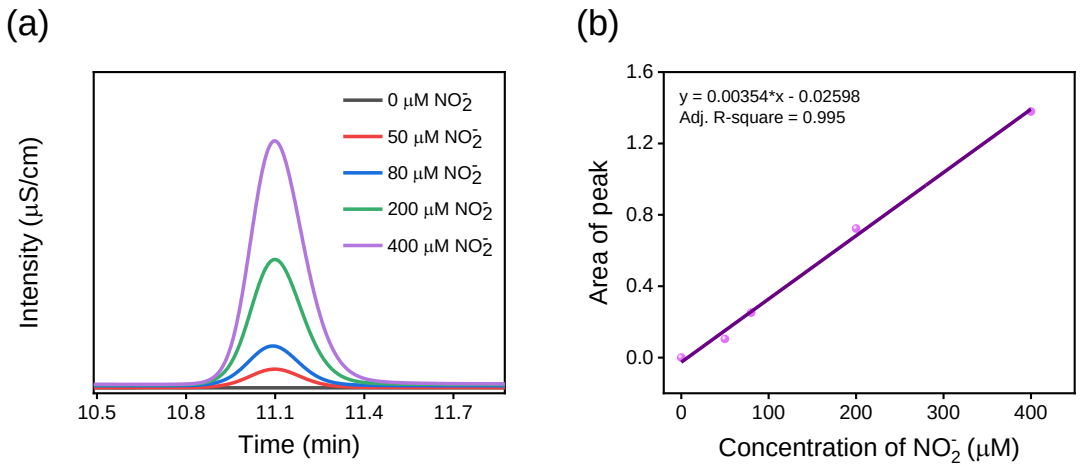

Figure. S19. (a) Ion-exchange chromatograms, and (b) Calibration curve plot for the estimation of NO_2^- ion.

Supplementary information **Figure S20.**

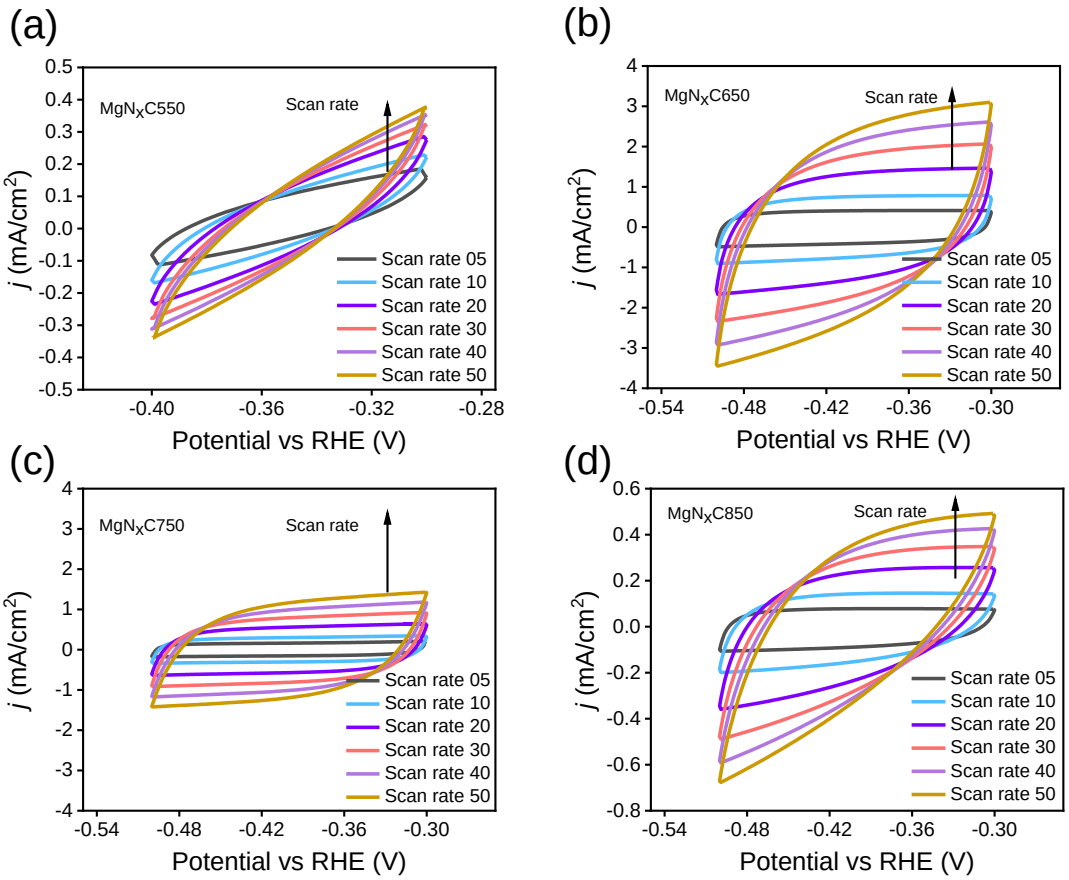

Figure. S20. Cyclic voltammetry curve signature of (a) MgNxC550, (b)MgNxC650, (c) MgNxC750 and (d) MgNxC850.

Supplementary information **Figure S21.**

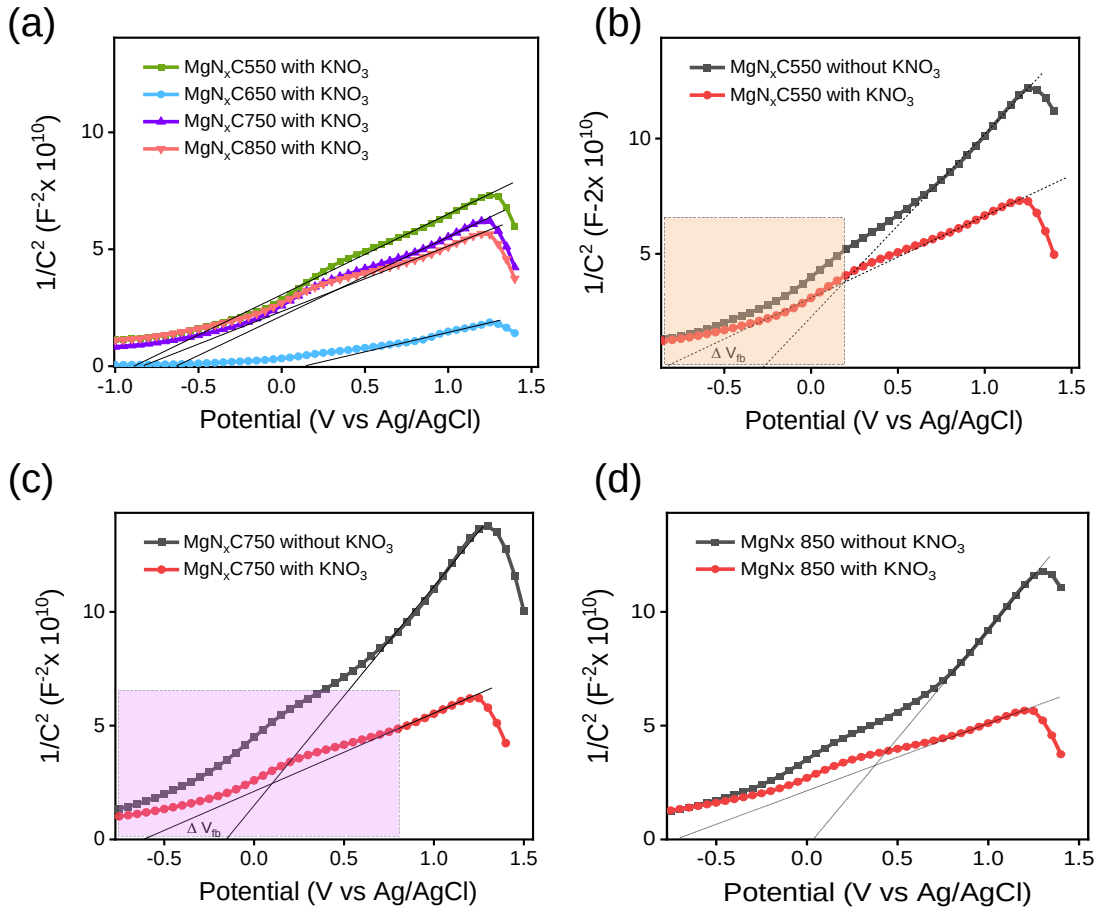

Figure. S21. (a) Mott-Schottky (M-S) plots of MgN_xC samples after introducing 1M KNO_3 in 1M KOH electrolyte medium. (b) comparison of deviation in the M-S plot before and after the addition of KNO_3 on MgN_xC550, (c) MgN_xC750, and (d) MgNxC850.

Supplementary information **Figure S22.**

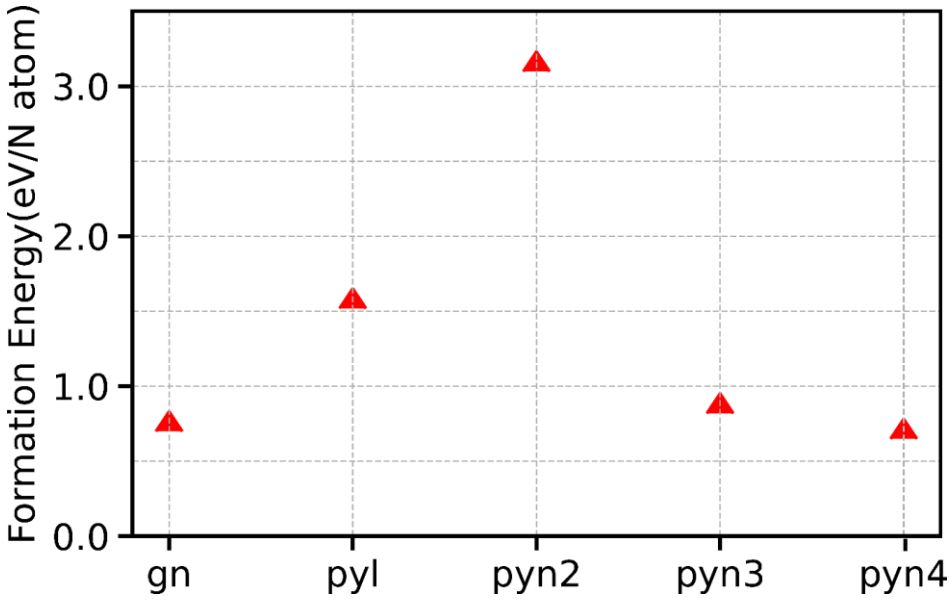

Figure. S22. Formation energies of N-doped structures showing g-N, pyridinic-3 (pyn3) and pyridinic-4 (pyn4) are relatively more stable than pyrrolic and pyridinic-2 (pyn2).

Supplementary information **Figure S23.**

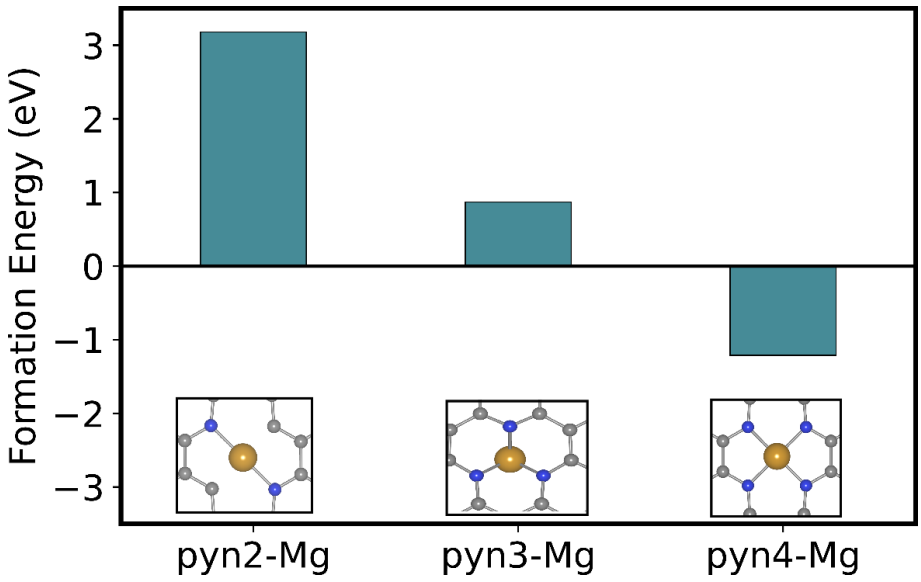

Figure. S23. Formation energy of Mg-SAC with Mg coordinated to two, three and four N atoms. Tetracoordinated Mg atoms are most stable forming the Mg-SAC substrate.

Supplementary information **Figure S24.**

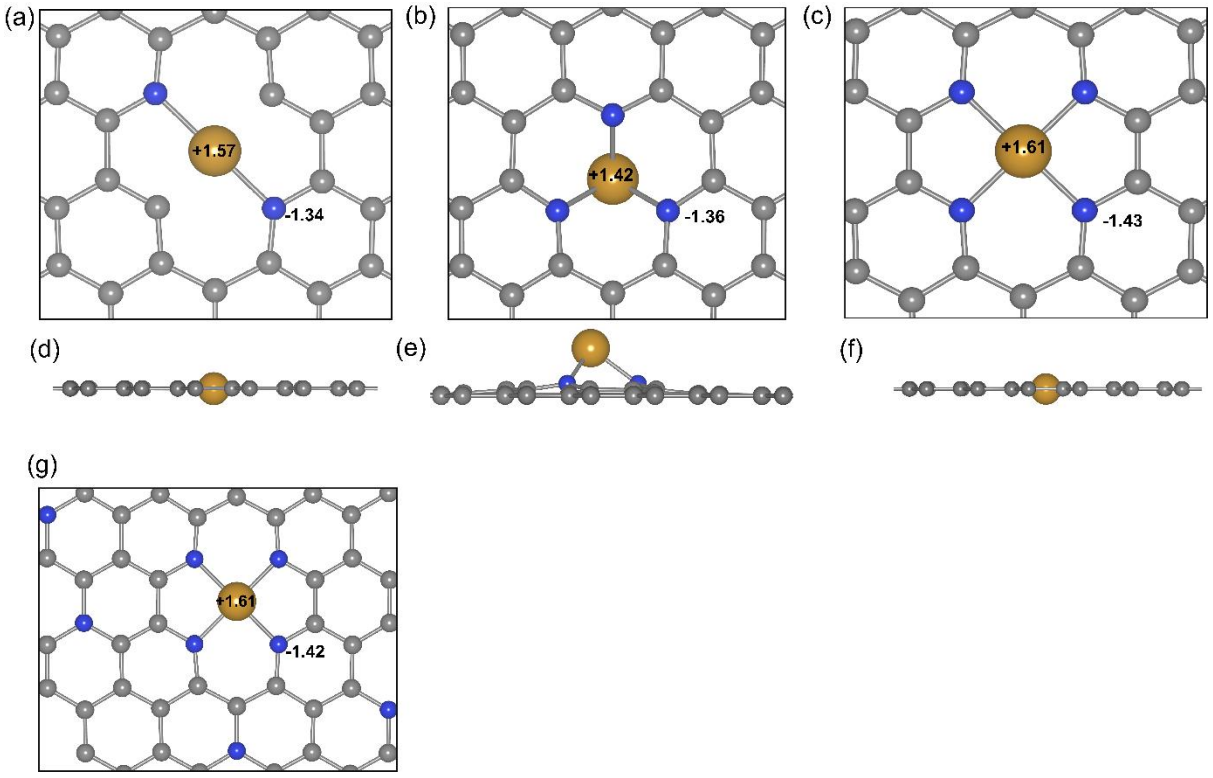

Figure. S24. Bad **Figure. S24.** Bader charge distributions of Mg and N atoms in the substrate. In plane Mg atoms in (a) pyn2 and (c)pyn4 show better charge transfer between Mg and N atoms. For (b) pyn3, Mg atom moves out of the plane, and (g) the final substrate structure.

Supplementary information **Figure S25.**

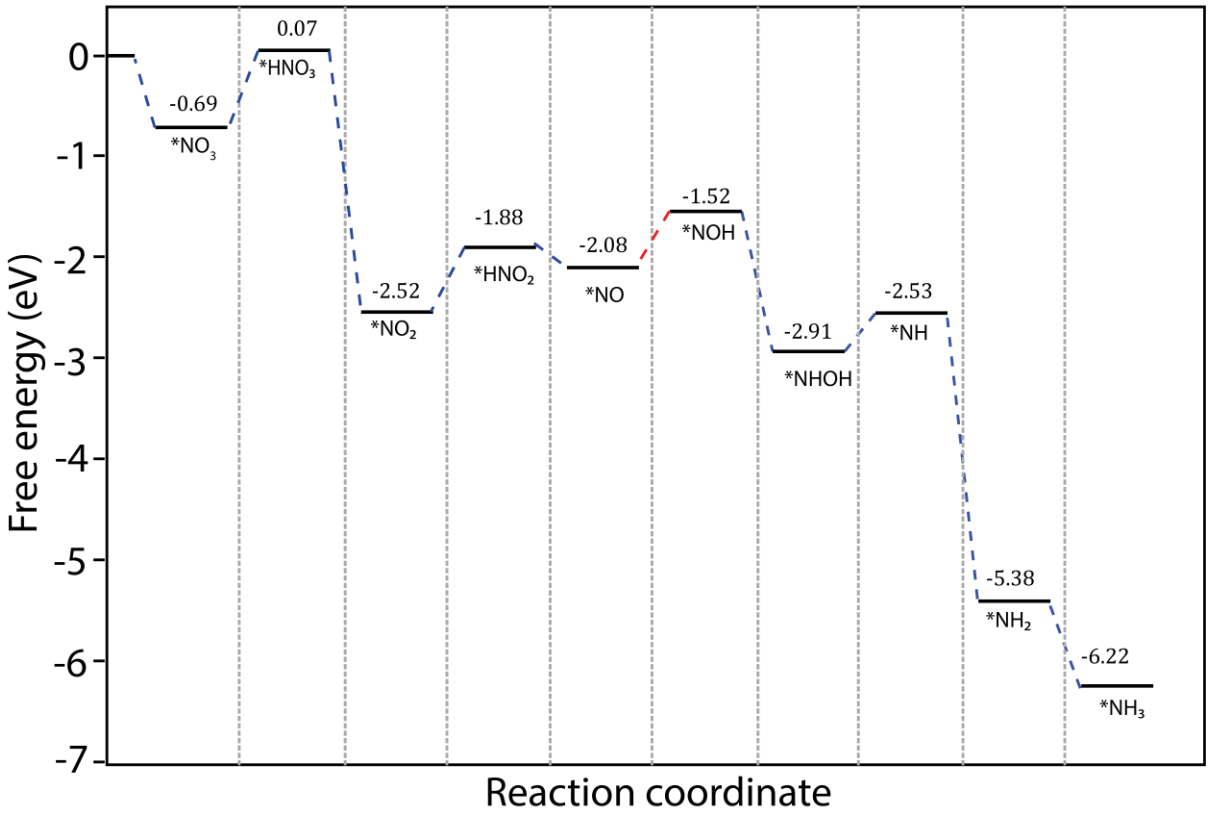

Figure. S25. Calculated free energy diagram for the NRA2 where, on *NO, hydrogenation takes place on oxygen atom. This step is thermodynamically uphill.

Supplementary information **Figure S26.**

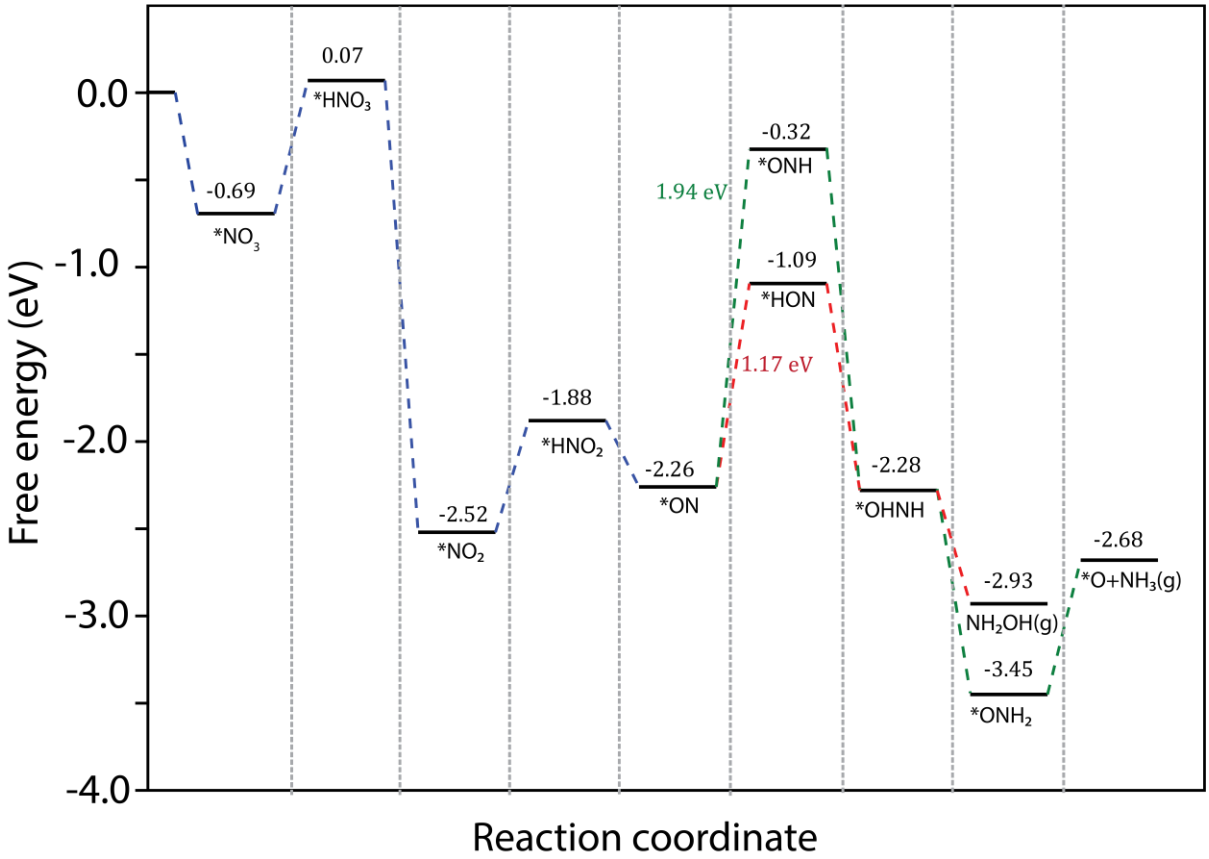

Figure. S26. Calculated free energy diagram for the NRA3 where, on *ON, hydrogenation takes place on O and N, leading to *HON and *ONH with thermodynamic potential barriers of 1.17 and 1.94 eV respectively.

Supplementary information **Figure S27.**

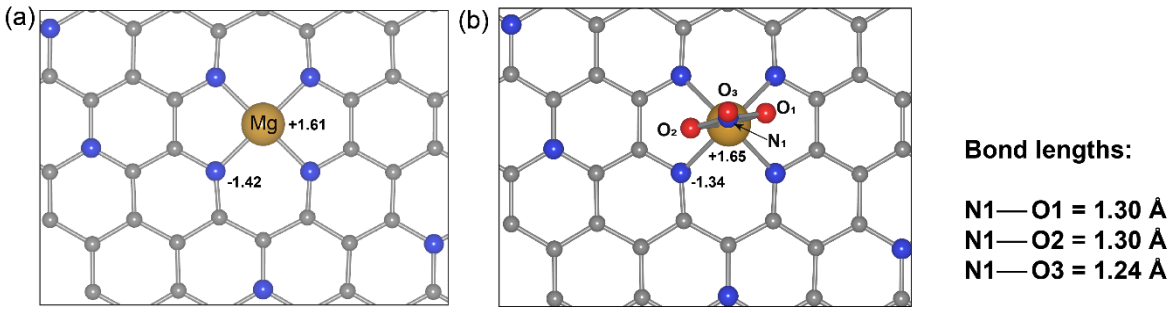

Figure. S27. Charge distribution on the substrate (a) before and (b) after adsorption of *NO_3 and the elongation of N-O bonds after *NO_3 adsorption.

Supplementary information **Figure S28.**

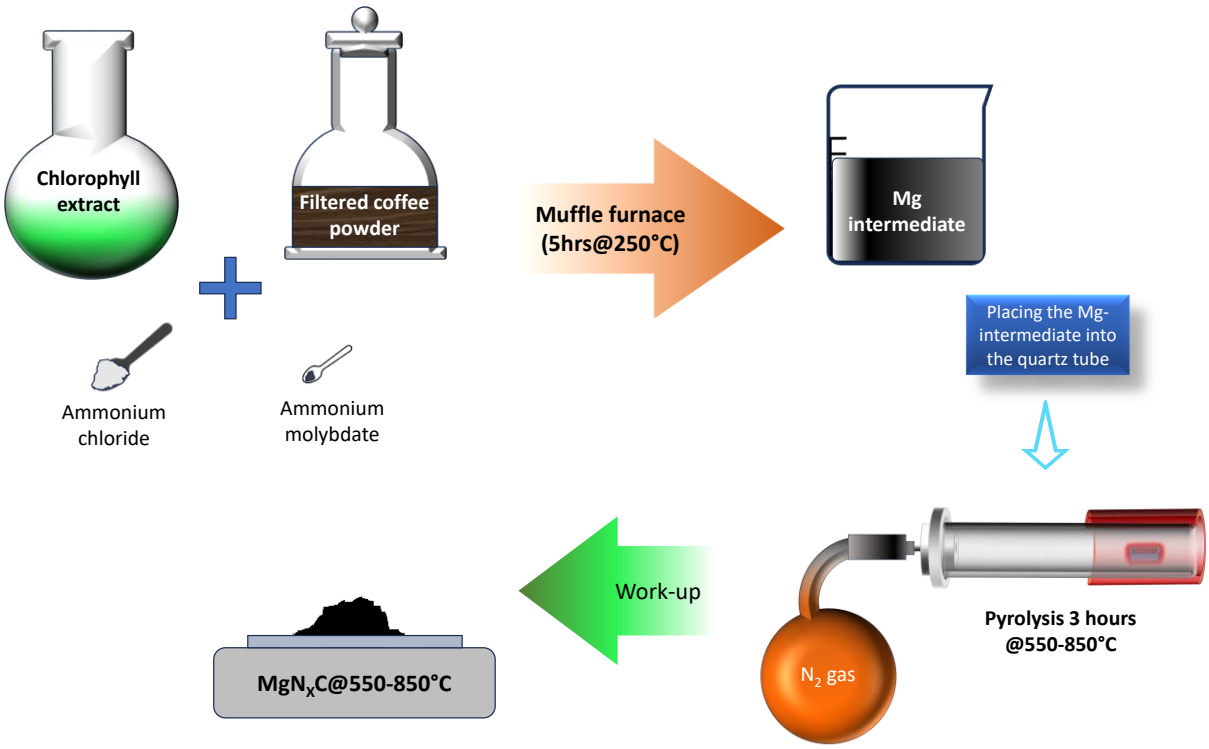

Figure. S28. Schematic diagram of Synthetic procedure of MgNxC catalyst at different temperatures.

Supplementary information **Figure S29.**

Figure. S29. Schematic diagram for chlorophyll extraction from spinach leaves at temperature of 80-85°C.

Supplementary information **Figure S30.**

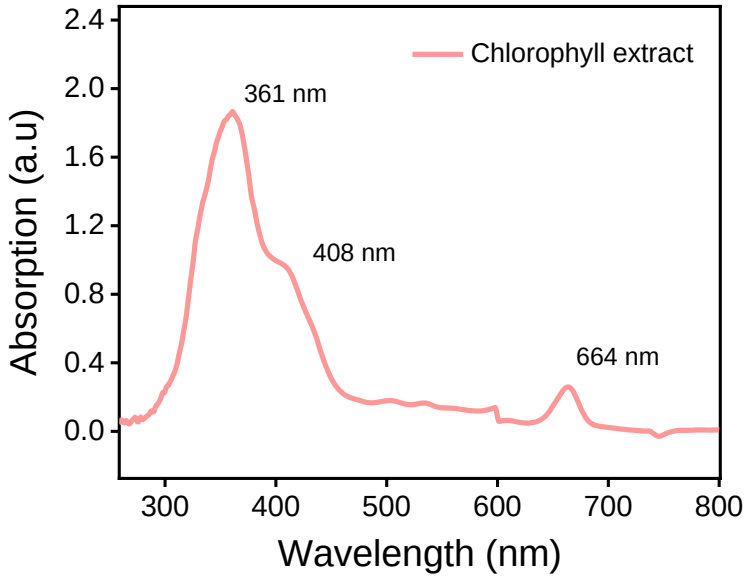

Figure. S30. UV-Visible spectra of extracted chlorophyll solution from Spinach leaves.

Supplementary information **Figure S31.**

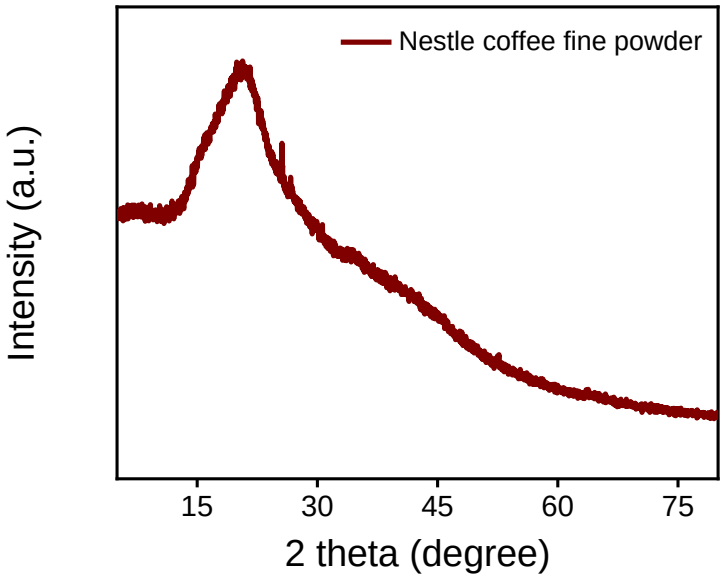

Figure. S31. X-Ray diffraction pattern of coffee powder after sieve filtration.

Supplementary information **Figure S32.**

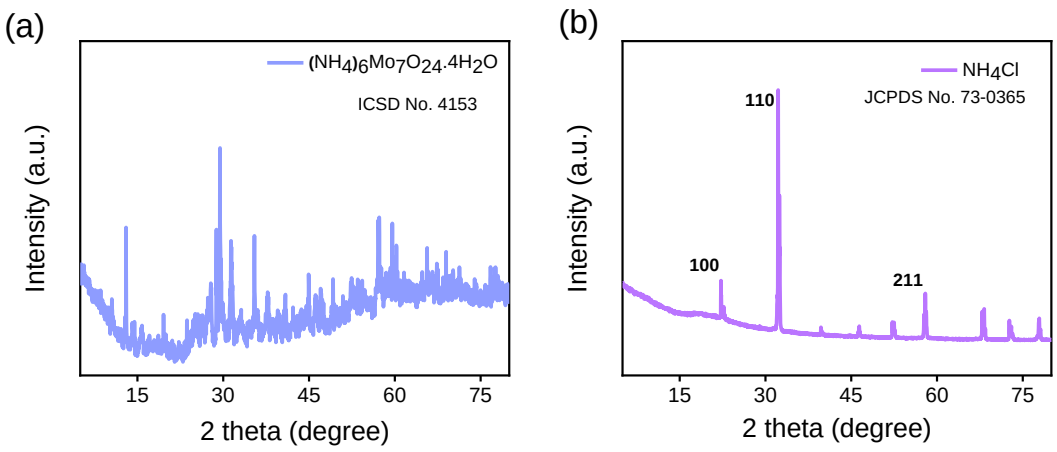

Figure. S32. X-Ray diffraction pattern (a) ammonium molybdate and (b) ammonium chloride.

Supplementary information **Figure S33.**

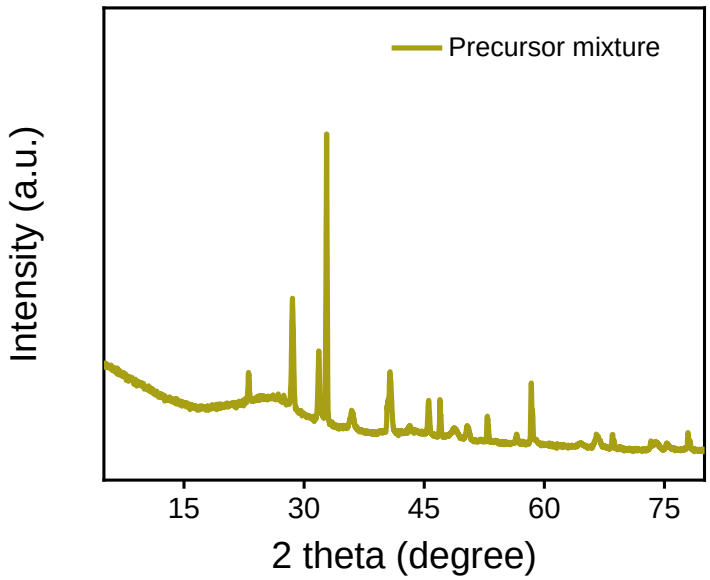

Figure. S33. X-Ray diffraction pattern of mixture of precursors (Chlorophyll solution + coffee powder+ ammonium chloride and ammonium molybdate.

Supplementary information **Figure S34.**

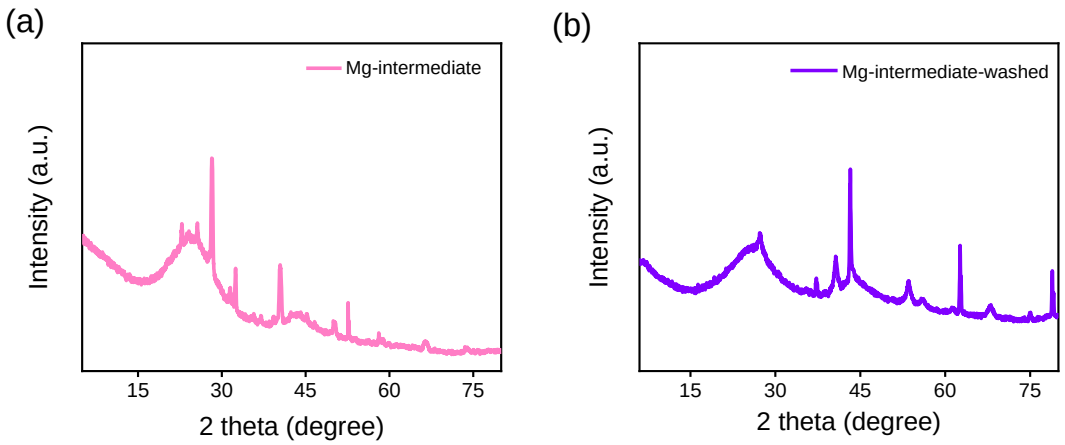

Figure. S34. X-Ray diffraction (a) product after muffle furnace (Mg-intermediate) and the (b) Mg-intermediate after washing.

Supplementary information **Figure S35.**

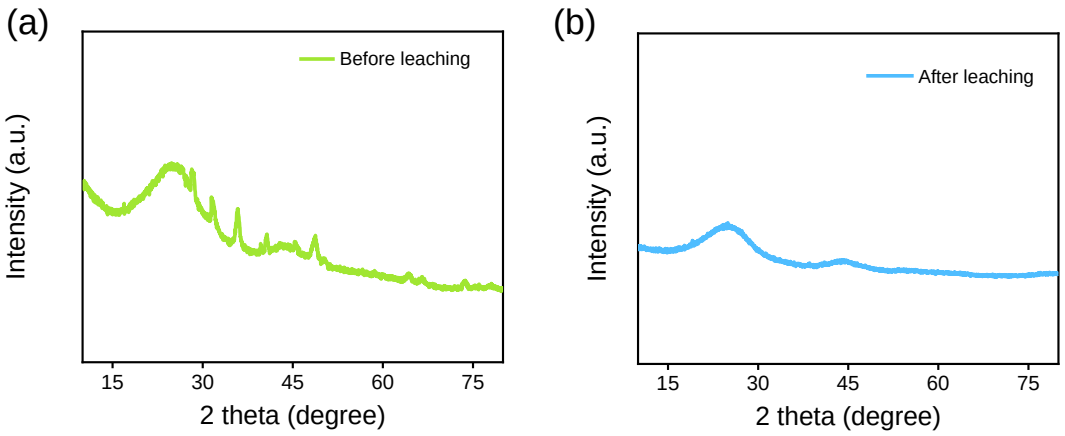

Figure. S35. X-ray diffraction pattern of a product after pyrolysis (a) before leaching (MgNxC650) and (b) after leaching (final product (MgNxC650) catalyst).

Supplementary information **Figure S36.**

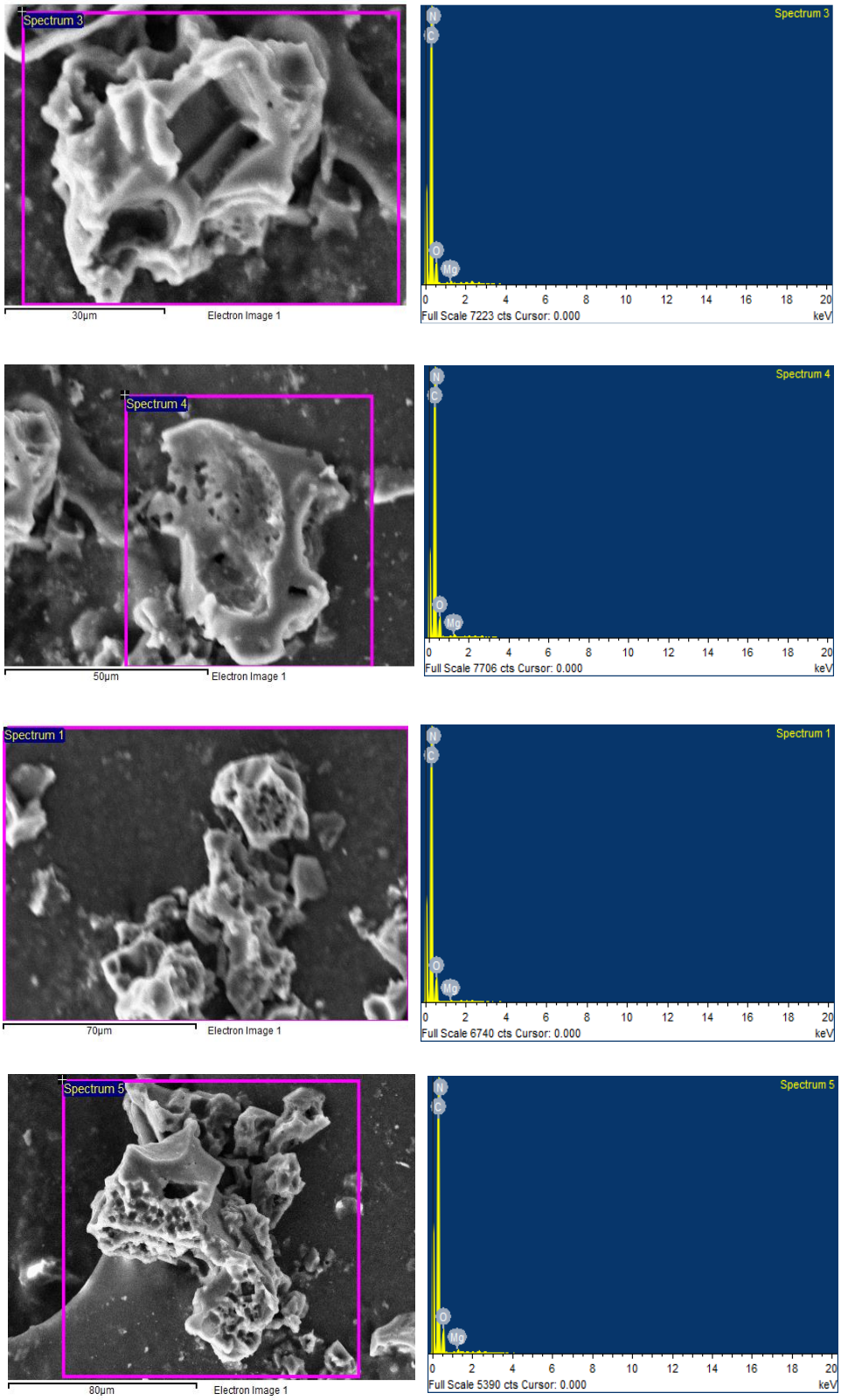

Figure. S36. SEM-EDS elemental spectra of final product (MgNxC650 catalyst) at different regions over a wide X-ray energy (keV) window.

Supplementary information **Figure S37.**

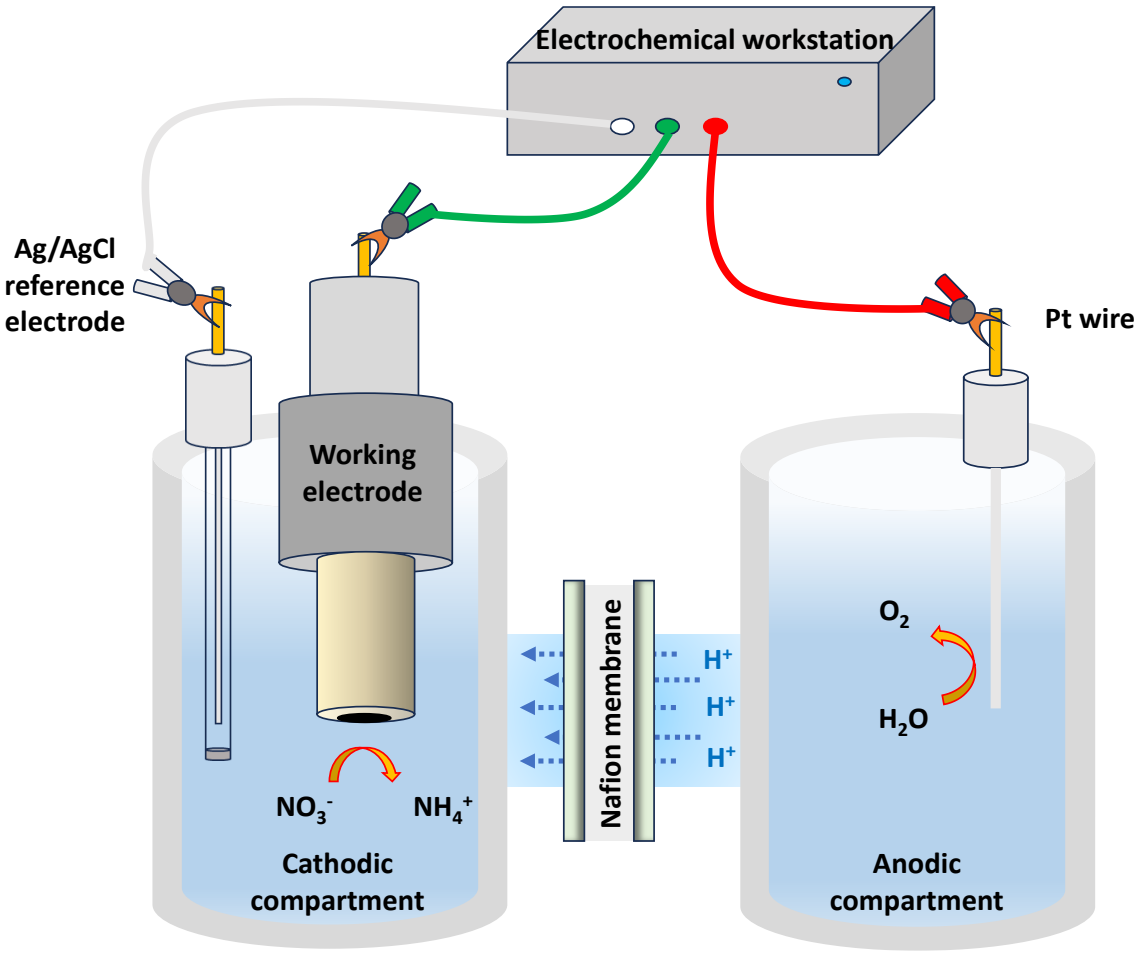

Figure. S37. Schematic diagram for electrochemical nitrate reduction working setup.